

| | | | | |
|---|---|--|--|--|
| REPORT DOCUMENTATION PAGE | | | Form Approved OMB No. 074-0188 | |
| Public reporting burden for this collection of information is estimated to average 1 hour per response, including the time for reviewing instructions, searching existing data sources, gathering and maintaining the data needed, and completing and reviewing this collection of information. Send comments regarding this burden estimate or any other aspect of this collection of information, including suggestions for reducing this burden to Washington Headquarters Services, Directorate for Information Operations and Reports, 1215 Jefferson Davis Highway, Suite 1204, Arlington, VA 22202-4302, and to the Office of Management and Budget, Paperwork Reduction Project (0704-0188), Washington, DC 20503 | | | | |
| 1. AGENCY USE ONLY (Leave blank) | | 2. REPORT DATE 7/20/2006 | | 3. REPORT TYPE AND DATES COVERED Final Performance Report 01/01/03-12/31/05 |
| 4. TITLE AND SUBTITLE Terahertz Electromagnetic Imaging of Dielectric Materials | | | 5. FUNDING NUMBERS F 49620-03-1-0185 | |
| 6. AUTHOR(S) Gabriella Pinter | | | | |
| 7. PERFORMING ORGANIZATION NAME(S) AND ADDRESS(ES) University of Wisconsin Milwaukee P.O. Box 413 Milwaukee, WI 53201-0413 | | | 8. PERFORMING ORGANIZATION REPORT NUMBER 144-LR79 | |
| 9. SPONSORING / MONITORING AGENCY NAME(S) AND ADDRESS(ES) AFOSR 875 North Rudolph St. Arlington, VA 22203 <i>Scott Wells</i> | | | 10. SPONSORING / MONITORING AGENCY REPORT NUMBER AFRL-SR-AR-TR-06-0394 | |
| 11. SUPPLEMENTARY NOTES | | | | |
| 12a. DISTRIBUTION / AVAILABILITY STATEMENT <i>Approved for public release; distribution unlimited</i> | | | | 12b. DISTRIBUTION CODE |
| 13. ABSTRACT (Maximum 200 Words) Theoretical and computational methodologies for the investigation of the propagation of high frequency ultrashort electromagnetic pulses in dielectric materials were developed. The models incorporated nonlinearly forced Debye and nonlinear Debye polarization dynamics and demonstrated the importance of taking into consideration nonlinear effects especially when the amplitude of the input signal was large. The development of a Brillouin precursor was demonstrated in linear and nonlinear models and its attenuation rate was analyzed. This study readily extends to include the imaging problem, i.e., the identification of electromagnetic and geometric properties of a hidden substance. Related to the interaction of electromagnetic waves with the dynamics of rubber-like materials, molecular based models for the dynamic extension and shear of elastomer rods and blocks were developed and analyzed. | | | | |
| 14. SUBJECT TERMS electromagnetic pulses, nonlinear polarization, precursors, imaging | | | | 15. NUMBER OF PAGES 14 |
| | | | | 16. PRICE CODE |
| 17. SECURITY CLASSIFICATION OF REPORT | 18. SECURITY CLASSIFICATION OF THIS PAGE | 19. SECURITY CLASSIFICATION OF ABSTRACT | 20. LIMITATION OF ABSTRACT | |

TERAHERTZ ELECTROMAGNETIC IMAGING OF DIELECTRIC MATERIALS

Gabriella A. Pinter
Department of Mathematical Sciences
University of Wisconsin, Milwaukee

1 Introduction

Research efforts were directed towards the understanding of high frequency (gigahertz and higher) ultrashort pulse propagation in dielectric materials for the purpose of extending current imaging capabilities and the assessment of safety standards. We formulated a full-wave variational Maxwell model that provides the theoretical and computational foundation for this problem. The model can incorporate linear and nonlinear polarization dynamics, and facilitates the comparison of the resulting phenomena. In particular, we were interested in temporal transients, like the Brillouin precursors, and how they changed their characteristics under different constitutive laws.

The results described first concern the theoretical foundations of this problem, and show that under fairly general conditions the model permits a unique weak solution that depends continuously on the input parameters.

An efficient numerical algorithm was developed for our extensive simulations and analysis based on different versions of the presented model. This algorithm can be extended readily to include the imaging problem, i.e., the identification of electromagnetic and geometric properties of a hidden substance.

We also investigated the interaction of electromagnetic waves with the dynamics of polymeric/viscoelastic materials. As a first step, we developed a molecular based multiscale model that correctly describes the characteristics (e.g., hysteresis) exhibited by these materials in dynamical extension and shear deformations. This model can then be coupled to the electromagnetic phenomena to provide a complete description of the problem. This research was joint work with H.T. Banks and N.G. Medhin from North Carolina State University.

2 Theoretical results

We consider a time-domain model for the propagation of high-intensity electromagnetic waves (e.g., laser beams) in dielectric materials. This work is a continuation of the efforts in the monograph [2], where the authors investigated a similar model using the full Maxwell's equations together with linear constitutive relations in a variational approach for the propagation of microwaves through dielectric layers. The variational approach facilitates the

incorporation of antenna sources in the model and provides an approximate computation of the electromagnetic transients like the Brillouin precursor. We extended the applicability of the results in [2] in the following sense: the model in the monograph contains a linear constitutive relationship describing material polarization in a convolution representation. Such a formulation includes Debye and Lorentz polarization models and is adequate to describe the interaction of microwaves with dielectric materials. However, the polarization mechanism cannot be assumed to be linear in the case of very high intensity electromagnetic waves, like lasers. Thus we developed theoretical results using a representation of the polarization by a nonlinear convolution. In particular, we take a physical model similar to that in [2], introduce a polarization law

$$P(t, z) = \int_0^t g(t - s, z)(E(s, z) + f(E(s, z)))ds, \quad (2.1)$$

and establish the well-posedness of the resulting system. This formulation can be interpreted as a generalization of the Debye or Lorentz polarization models in the sense that the polarization dynamics is driven by a nonlinear function of the electric field. We show the global existence-uniqueness and continuous dependence on data of weak solutions under general assumptions on the nonlinearity f . These conditions are satisfied by a number of locally polynomial nonlinearities proposed in the nonlinear optics literature (e.g., see the “second order” optical models involving cubic nonlinearities in [10, 11].) Based on these theoretical results, rigorous computational methods can be developed for the forward problem and subsequently for the associated inverse problems. After a detailed description of the specific problem studied we refer to [3, 7] for the technical details of the proofs.

We consider Maxwell’s equations applied to a specific physical problem as depicted in Figure 1. An infinite slab of material is interrogated by a normally incident polarized plane wave windowed pulse originating at an antenna source $z = 0$ in free space $\Omega_0 = [0, z_1]$. The slab of material in $\Omega = [z_1, z_2]$ is assumed to be homogeneous in the directions orthogonal to the direction z of propagation of the plane wave. Under these assumptions the strength of the electric and magnetic fields in Ω and Ω_0 can be represented by the scalar functions $E(t, z)$ and $H(t, z)$, respectively. One can readily eliminate the magnetic field from the full Maxwell equations to arrive at the strong formulation of the problem (for a detailed derivation see [2])

$$\mu_0 \epsilon \ddot{E} + \mu_0 I_\Omega(z) \ddot{P} + \mu_0 \sigma \dot{E} - E'' = -\mu_0 \dot{J}_s \quad 0 < z < z_2, \quad t > 0, \quad (2.2)$$

$$\frac{1}{c} \frac{\partial E}{\partial t} - \frac{\partial E}{\partial z} \Big|_{z=0} = 0 \quad t > 0, \quad (2.3)$$

$$E(t, z_2) = 0 \quad t > 0, \quad (2.4)$$

$$E(0, z) = \Phi(z), \quad \dot{E}(0, z) = \Psi(z) \quad 0 < z < z_2, \quad (2.5)$$

where P denotes the polarization and I_Ω is the indicator function

$$I_\Omega(z) = \begin{cases} 0 & \text{if } 0 < z < z_1 \\ 1 & \text{if } z_1 \leq z \leq z_2, \end{cases},$$

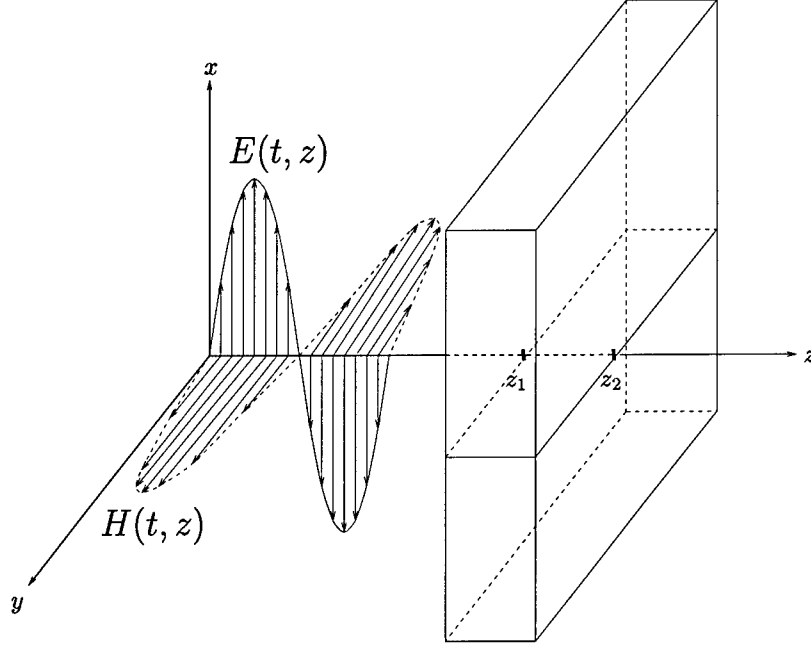


Figure 1: Geometry of the physical problem

where $z_1 < 1$ is the front boundary of the slab and z_2 is the (sometimes unknown in interrogation problems) back boundary (see Figure 1). We note that an absorbing boundary condition is placed at $z = 0$ to prevent the reflection of waves. We assume that there is a supraconductive backing on the slab at $z = z_2$ and specify the boundary conditions accordingly. Equation (2.2) can be given in the form

$$\frac{\epsilon}{\epsilon_0} \ddot{E} + \frac{1}{\epsilon_0} I_\Omega(z) \ddot{P} + \frac{1}{\epsilon_0} \sigma \dot{E} - c^2 E'' = -\frac{1}{\epsilon_0} j_s,$$

where $\epsilon = \epsilon_0(1 + (\epsilon_r - 1)I_\Omega)$, and $c^2 = \frac{1}{\epsilon_0 \mu_0}$. We denote $\frac{\epsilon}{\epsilon_0}$ by $\tilde{\epsilon}_r$.

We assume that the frequency of the interrogating wave is so high that the dependence of the polarization on the electric field can no longer be adequately described by a linear constitutive law. Specifically, we consider a polarization mechanism that depends on the strength of the electric field in the convolution in (2.1). Thus

$$\begin{aligned} \ddot{P}(t, z) &= \int_0^t \ddot{g}(t-s, z) f(E(s, z)) ds + g(0, z) \frac{\partial}{\partial t} f(E(t, z)) + \dot{g}(0, z) f(E(t, z)) \\ &+ \int_0^t \ddot{g}(t-s, z) E(s, z) ds + g(0, z) \dot{E}(t, z) + \dot{g}(0, z) E(t, z), \end{aligned}$$

where $f : \mathbb{R} \rightarrow \mathbb{R}$ is a nonlinear (not necessarily small) perturbation of the linear mechanism. This yields the strong form of the equation

$$\tilde{\epsilon}_r \ddot{E}(t, z) + \frac{1}{\epsilon_0} I_\Omega(z) (\sigma(z) + g(0, z)) \dot{E}(t, z)$$

$$\begin{aligned}
& + \frac{1}{\epsilon_0} I_\Omega(z) \dot{g}(0, z) E(t, z) + \int_0^t \frac{1}{\epsilon_0} I_\Omega(z) \ddot{g}(t-s, z) E(s, z) ds \\
& + \frac{1}{\epsilon_0} I_\Omega(z) \dot{g}(0, z) f(E(t, z)) + \int_0^t \frac{1}{\epsilon_0} I_\Omega(z) \ddot{g}(t-s, z) f(E(s, z)) ds \\
& + \frac{1}{\epsilon_0} I_\Omega(z) g(0, z) \frac{d}{dt} f(E(t, z)) - c^2 E''(t, z) = -\frac{1}{\epsilon_0} \dot{J}_s(t, z), \quad 0 < z < z_2. \quad (2.6)
\end{aligned}$$

In the physical problem z_2 is assumed to be unknown, and it is desirable to estimate it from given data. Since the existence proof is constructive in the sense that the numerical method we use to solve this problem (for both forward and inverse problems) follows the theoretical arguments, it is desirable to convert the problem to a fixed spatial domain, e.g., $[0, 1]$, as explained in [2]. We then do not need to update the spatial discretization and the basis functions for different z_2 , but the same numerical framework can be used throughout the optimization procedure in the inverse problems.

To this end we first multiply (2.6) by ϕ , where $\phi \in H^1(0, z_2)$ and integrate from 0 to z_2 using integration by parts in the last term in the left. Then we introduce a change of variable by letting

$$\tilde{z} = h(z) = \begin{cases} z_1 & \text{if } 0 < z < z_1 \\ z_1 + (z - z_1) \frac{1-z_1}{z_2-z_1} & \text{if } z_1 \leq z \leq z_2, \end{cases}$$

i.e., $h(z) = z + (\zeta - 1)(z - z_1)I_{[z_1, z_2]}(z)$ with $\zeta = \frac{1-z_1}{z_2-z_1}$. Then $h'(z) = 1 + (\zeta - 1)I_\Omega(z)$ and $\tilde{h}'(\tilde{z}) = 1 + (\zeta - 1)I_{\tilde{\Omega}}(\tilde{z})$, where $\tilde{\Omega} = [z_1, 1]$ and we adopt the notation that $\tilde{E}, \tilde{h}, \tilde{\phi}, \tilde{g}$, etc., are the maps E, h, ϕ, g , etc., after they have been mapped from the domain $[0, z_2]$ to the domain $[0, 1]$. Using this transformation we obtain

$$\begin{aligned}
& \langle \frac{1}{\tilde{h}'(\tilde{z})} \tilde{\epsilon}_r \ddot{\tilde{E}}(t, \cdot), \tilde{\varphi}(\tilde{z}) \rangle + \langle \frac{1}{\tilde{h}'(\tilde{z})} \frac{1}{\epsilon_0} I_{\tilde{\Omega}}(\tilde{z}) (\tilde{\sigma} + \tilde{g}(0, \cdot)) \dot{\tilde{E}}(t, \cdot), \tilde{\varphi}(\tilde{z}) \rangle \\
& + \langle \frac{1}{\tilde{h}'(\tilde{z})} \frac{1}{\epsilon_0} I_{\tilde{\Omega}}(\tilde{z}) \dot{\tilde{g}}(0, \cdot) \tilde{E}(t, \cdot), \tilde{\varphi}(\tilde{z}) \rangle + \langle \frac{1}{\tilde{h}'(\tilde{z})} \int_0^t \frac{1}{\epsilon_0} I_{\tilde{\Omega}}(\tilde{z}) \ddot{\tilde{g}}(t-s, \cdot) \tilde{E}(s, \cdot) ds, \tilde{\varphi}(\tilde{z}) \rangle \\
& + \langle \frac{1}{\tilde{h}'(\tilde{z})} \frac{1}{\epsilon_0} I_{\tilde{\Omega}}(\tilde{z}) \dot{\tilde{g}}(0, \cdot) f(\tilde{E}(t, \cdot)), \tilde{\varphi}(\tilde{z}) \rangle + \langle \frac{1}{\tilde{h}'(\tilde{z})} \int_0^t \frac{1}{\epsilon_0} I_{\tilde{\Omega}}(\tilde{z}) \ddot{\tilde{g}}(t-s, \cdot) f(\tilde{E}(s, \cdot)) ds, \tilde{\varphi}(\tilde{z}) \rangle \\
& + \langle \frac{1}{\tilde{h}'(\tilde{z})} \frac{1}{\epsilon_0} I_{\tilde{\Omega}}(\tilde{z}) \tilde{g}(0, \cdot) \frac{d}{dt} f(\tilde{E}(t, \cdot)), \tilde{\varphi}(\tilde{z}) \rangle + \langle c^2 \tilde{h}' \tilde{E}'(t, \cdot), \tilde{\varphi}' \rangle + c \dot{\tilde{E}}(t, 0) \tilde{\varphi}(0) \\
& = -\langle \frac{1}{\tilde{h}'(\tilde{z})} \frac{1}{\epsilon_0} \dot{\tilde{J}}_s(t, \cdot), \tilde{\varphi}(\tilde{z}) \rangle, \quad (2.7)
\end{aligned}$$

where $\langle \cdot, \cdot \rangle$ is the $L^2(0, 1)$ inner product. This effectively maps our system to a fixed reference domain $[0, 1]$ and we use this form to define the weak solution of the problem. We let $H = L^2(0, 1)$, $V = H_R^1(0, 1) = \{\phi \in H^1(0, 1) | \phi(1) = 0\}$ leading to the Gelfand triple ([15, 20]) $V \hookrightarrow H \hookrightarrow V^*$. We say that $E \in L^\infty(0, T; V)$ with $\dot{E} \in L^2(0, T; H)$, $\ddot{E} \in L^2(0, T; V^*)$, is a weak solution if it satisfies for every $\varphi \in V$

$$\begin{aligned}
& \langle \bar{\varepsilon}_r \ddot{E}, \varphi \rangle_{V^*, V} + \langle \gamma \dot{E}, \varphi \rangle + \langle \beta E, \varphi \rangle + \langle \int_0^t \alpha(t-s, \cdot) E(s, \cdot) ds, \varphi \rangle \\
& + \langle \beta f(E), \varphi \rangle + \langle \int_0^t \alpha(t-s, \cdot) f(E(s, \cdot)) ds, \varphi \rangle + \langle \hat{\gamma} \frac{d}{dt} f(E), \varphi \rangle \\
& + \langle c^2 h' E', \varphi' \rangle + c \dot{E}(t, 0) \varphi(0) = \langle \mathcal{J}(t, \cdot), \varphi \rangle_{V^*, V}
\end{aligned} \tag{2.8}$$

and

$$E(0, z) = \Phi(z), \quad \dot{E}(0, z) = \Psi(z), \tag{2.9}$$

where in (2.8) we drop the overtilda on variables and functions for simplification of notation and for $\tilde{z} \in [0, 1]$, we define

$$\begin{aligned}
\alpha(t, \tilde{z}) &= \frac{1}{\tilde{h}'(\tilde{z})} \frac{1}{\epsilon_0} I_{\tilde{\Omega}}(\tilde{z}) \ddot{g}(t, \tilde{z}), \\
\beta(\tilde{z}) &= \frac{1}{\tilde{h}'(\tilde{z})} \frac{1}{\epsilon_0} I_{\tilde{\Omega}}(\tilde{z}) \dot{g}(0, \tilde{z}), \\
\gamma(\tilde{z}) &= \frac{1}{\tilde{h}'(\tilde{z})} \frac{1}{\epsilon_0} I_{\tilde{\Omega}}(\tilde{z}) (\tilde{\sigma}(\tilde{z}) + \tilde{g}(0, \tilde{z})), \\
\hat{\gamma}(\tilde{z}) &= \frac{1}{\tilde{h}'(\tilde{z})} \frac{1}{\epsilon_0} I_{\tilde{\Omega}}(\tilde{z}) \tilde{g}(0, \tilde{z}), \\
\mathcal{J}(t, \tilde{z}) &= -\frac{1}{\tilde{h}'(\tilde{z})} \frac{1}{\epsilon_0} \dot{J}_s(t, \tilde{z}), \\
\bar{\varepsilon}_r &= \frac{1}{\tilde{h}'(\tilde{z})} \tilde{\varepsilon}_r.
\end{aligned}$$

We note that since $\frac{1}{\tilde{h}'(z)} > 0$ is a piecewise constant function, the inclusion of this term in $\alpha, \beta, \gamma, \hat{\gamma}, \bar{\varepsilon}_r, \mathcal{J}$ is essentially equivalent to using a modified ϵ_0 . In developing the theoretical existence result we can also make the simplifying assumption that $\bar{\varepsilon}_r = 1$ without loss of generality. (This, of course, is not true for computational efforts.) Our goal is to establish the existence and uniqueness of weak solutions.

We make the following assumptions:

A1) The functions $\beta, \gamma, \hat{\gamma} \in L^\infty(0, 1)$ with

$$|\beta(z)| \leq L_1, \quad |\hat{\gamma}(z)| \leq L_2.$$

A2) The function α is bounded on $[0, T] \times (0, 1)$ with

$$|\alpha(t, z)| \leq L_3.$$

- A3) $g(0, z) \geq 0, \sigma(z) \geq 0$. (We note that this assumption implies that $\gamma(z) \geq 0, \hat{\gamma}(z) \geq 0$ for every $z \in [0, 1]$.)
- A4) The nonlinear function $f : \mathbb{R} \rightarrow \mathbb{R}$ is C^1 , with $f(0) = 0$, and $f'(z) > 0$ for all $z \in \mathbb{R}$. f is also assumed to be affine at infinity, i.e., there exist constants R, L_R and K_R such that for every $|x| > R$, $|f(x)| \leq L_R|x| + K_R$.

We proved the following theorem:

Theorem 2.1 *Under assumptions A1)-A4) the system (2.8)-(2.9) has a weak solution for any $\Phi \in V, \Psi \in H$ and $\mathcal{J} \in H^1(0, T; V^*)$. The weak solution depends continuously on initial conditions and the source term, i.e., the mapping $(\Phi, \Psi, \mathcal{J}) \rightarrow (E, \dot{E})$ is continuous from $V \times H \times H^1(0, T; V^*)$ to $C(0, T; H) \times L^2_{weak}(0, T; H)$.*

Details of the proof can be found in [3].

The theoretical results are an initial effort in developing a foundation for nonlinear electromagnetics and the needed computational methods for such. The potential applications of nonlinear optics with light as an information carrier are widespread and are the basis of optical information technology and the use of optical fibers. They are of increasing importance with the development of materials (e.g., GaAs, InP, KNbO₃) which possess outstanding nonlinear optical and electro-optical properties [11]. Our interests arise from the potential of using interrogating input pulses in the IR range (terahertz) in imaging and more specifically in detection algorithms.

Nonlinear optical effects are usually described through nonlinear polarization laws [10] and many of these laws can be formulated in the framework above where we treat rather general nonlinearities. These include locally polynomial nonlinearities (e.g., so-called third order and higher effects [10, 11]) that are bounded as the magnitude of the E field saturates polarization mechanisms (e.g., the material "freezes" dielectrically at high field values). The assumption that the nonlinearity is increasing with the magnitude of the E field is again a realistic one.

We consider full wave propagation (as opposed to the popular paraxial approximate models [10] found widely in the literature), even here there are some tacit assumptions that may result in limiting approximations to phenomena that actually occur in nonlinear materials. Specifically, the one-dimensional model formulated in this section depends on the tacit assumption that the polarization field \bar{P} in the dielectric remains parallel to the electric field \bar{E} . Even then, the usual Maxwell equation $\nabla \cdot \bar{D} = 0$ along with the constitutive law $\bar{D} = \epsilon_0 \epsilon_r \bar{E} + f_1(P) \bar{P}$ need not result in $\nabla \cdot \bar{E} = 0$. This is important in deriving the second order form of Maxwell's equation where the identity $\nabla \times \nabla \times \bar{E} = \nabla(\nabla \cdot \bar{E}) - \nabla^2 \bar{E}$ results in the simple Laplacian only if $\nabla \cdot \bar{E} = 0$ or one assumes this term is negligible as often done in nonlinear optics ([10] p.54-60). Even with some obvious inadequacies, the model considered here does facilitate treatment of a number of mechanisms of interest, including Debye and Lorentz materials that are driven by nonlinear E field inputs, e.g., $\dot{P} + \frac{1}{\tau}P = f(E)$.

3 Numerical algorithm and simulations

Our models incorporate different linear and nonlinear polarization mechanisms which influence the propagation characteristics. First we study a linear Debye model [12], given by

$$\tau \dot{P} + P = \varepsilon_0(\varepsilon_s - \varepsilon_\infty)E, \quad t > 0, \quad (3.10)$$

and then extend it to a nonlinearly forced Debye and a mechanistically nonlinear Debye model. Our computational framework is based on a variational formulation of Maxwell's equations described in the previous section.

Our focus here is on understanding the propagation characteristics of pulses with different carrier frequencies, and for this purpose we set up a simplified model. However, we note that this simplified formulation can be readily extended to treat interfaces and the more general inverse problems. We consider an infinite (in the x and y direction) slab of homogeneous material of width ℓ with faces parallel to the xy plane. However, here we place an antenna inside the material, usually in the middle. The input signal is a planar electromagnetic wave polarized with oscillations in the xz plane only. The electromagnetic field \vec{E} is reduced to one nontrivial component, in the x direction, at all points of the slab, and it is homogeneous in intensity in the x and y directions.

For computational purposes we scale the time variable by a factor of c and polarization P by a factor of $1/\varepsilon_0$, i.e., we let $\tilde{E} = E(ct)$, $\tilde{P} = 1/\varepsilon_0 P(ct)$. We express \tilde{P} from (3.10) and substitute it into the weak formulation of the model. The new equations in the scaled variables are

$$\begin{aligned} \langle \varepsilon_r \ddot{\tilde{E}}, \varphi \rangle + \langle (\eta\sigma + \varepsilon_d\lambda) \dot{\tilde{E}}, \varphi \rangle + \langle \lambda^2 \tilde{P}, \varphi \rangle - \langle \varepsilon_d \lambda^2 \tilde{E}, \varphi \rangle + \langle \tilde{E}', \varphi' \rangle + \sqrt{\varepsilon_s} \dot{\tilde{E}}(0) \varphi(0) \\ + \sqrt{\varepsilon_s} \dot{\tilde{E}}(\ell) \varphi(\ell) = -\eta \langle \dot{\tilde{J}}_s, \varphi \rangle \end{aligned} \quad (3.11)$$

$$\langle \dot{\tilde{P}} + \lambda \tilde{P}, \varphi \rangle = \langle \varepsilon_d \lambda \tilde{E}, \varphi \rangle, \quad (3.12)$$

where we introduced the notation $\varepsilon_d = \varepsilon_s - \varepsilon_\infty$, $\lambda = \frac{1}{ct}$ and $\eta = \mu_0 c$. We discretize the problem in the space variable using a first order Galerkin finite element approximation. We divide the interval $[0, \ell]$ into N equal subintervals at the points $z = jh$, $j = 0, \dots, N$, where $h = \ell/N$, and construct standard piecewise linear splines $\phi_j^N(z)$. The finite dimensional approximating subspaces to V will be taken to be $V^N = \{\phi_0^N, \phi_1^N, \dots, \phi_N^N\}$. Now we approximate $E(t, z)$ and $P(t, z)$ in this space as

$$E(t, z) \approx E^N(t, z) = \sum_{j=0}^N e_j^N(t) \phi_j^N(z), \quad (3.13)$$

$$P(t, z) \approx P^N(t, z) = \sum_{j=0}^N p_j^N(t) \phi_j^N(z). \quad (3.14)$$

We choose the space of test functions to be V^N also, and thus we find that (3.11)-(3.12) lead to

$$\varepsilon_r M \ddot{e} + ((\eta\sigma + \varepsilon_d\lambda)M + \sqrt{\varepsilon_s}BD)\dot{e} + \lambda^2 Mp + (K - \lambda^2 \varepsilon_d M)e = -\eta \mathcal{J}, \quad (3.15)$$

$$M\dot{p} = -\lambda Mp + \varepsilon_d \lambda M e \quad (3.16)$$

where $e = (e_0^N, e_1^N, \dots, e_N^N)^T$, $p = (p_0^N, p_1^N, \dots, p_N^N)^T$, $\mathcal{J} = (\mathcal{J}_0, \dots, \mathcal{J}_N)^T$, with $\mathcal{J}_i = \langle \dot{J}_s, \phi_i \rangle$, $i = 0, \dots, N$, and

$$M_{ij} = \langle \phi_i, \phi_j \rangle = \int_0^\ell \phi_i(z) \phi_j(z) dz,$$

$$K_{ij} = \langle \phi_i', \phi_j' \rangle = \int_0^\ell \phi_i'(z) \phi_j'(z) dz.$$

Here BD denotes a matrix with $BD_{00} = BD_{NN} = 1$, while all other elements of the matrix are 0. We now employ a second order central difference approximation in the time variable to solve (3.15). We take

$$\ddot{e}(t^n) = \ddot{e}^n \approx \frac{e^{n+1} - 2e^n + e^{n-1}}{\Delta t^2}, \quad \dot{e}(t^n) = \dot{e}^n \approx \frac{e^{n+1} - e^{n-1}}{2\Delta t}$$

and

$$e(t^n) = e^n \approx \frac{e^{n+1} + e^n + e^{n-1}}{4}.$$

Now the Galerkin approximation (3.15) reduces to a linear equation that can be solved for e^{n+1} given e^n, e^{n-1} and p^n . We have initial condition $e^0 = 0$ and we approximate $e^1 \approx -\eta \frac{\Delta t^2}{2\varepsilon_r} \dot{J}_s(0, z)$. To obtain p^n we solve (3.16) using a Crank-Nicholson method. This approximation method is overall $\mathcal{O}(h^2)$ when $\Delta t = \mathcal{O}(h)$. We also note that the method is unconditionally stable.

We remark that our model is well-posed theoretically for various different linear and non-linear polarization mechanisms. The input pulse has the form $A \sin^3(\omega t) \chi_{[0, t_f]}(t) \delta(z - z_0)$, where A is the amplitude of the signal, and z_0 denotes the location where it is generated inside the material. We use a few (typically 4 to 7) whole periods of this signal, i.e., t_f is an integer multiple of $2\pi/\omega$. In the first set of experiments we observed the onset and propagation characteristics of the Brillouin precursors in the case when a linear Debye polarization mechanism is assumed. We find that in the 1-10 GHz frequency range the peak amplitude of the transient field is attenuated at a much slower rate in relation to propagation distance than the amplitude of the carrier frequency (see Figures 2 and 3). Indeed, a closer analysis of the attenuation rate reveals that while the carrier frequency decays exponentially, the attenuation of the transient is only algebraic, and proportional to approximately $x^{-0.62}$ in the 1 GHz case, and $x^{-0.59}$ in the 10 GHz case. This is in accordance with the results reported in [1] and the theoretical considerations based on asymptotic analysis in [17].

In the 0.1 to 1 THz regime the carrier frequency does not propagate inside the material, only the precursor enters. The attenuation rate of the amplitude of the leading transient with respect to propagation length in the 1 THz case is approximately proportional to $x^{-1.59}$.

Next we take a nonlinearly forced Debye polarization model given by

$$\tau \dot{P} + P = \varepsilon_0 \varepsilon_d E + f(E), \quad (3.17)$$

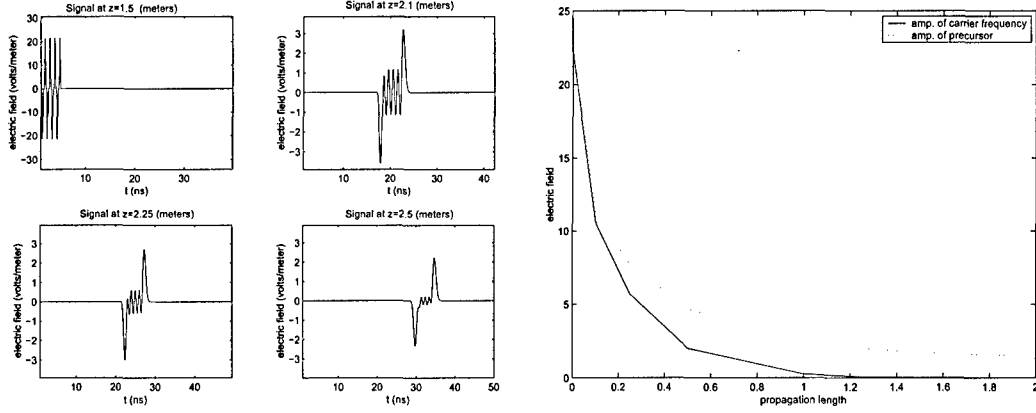


Figure 2: (left) The electric field recorded at the antenna and at 0.6, 0.75 and 1 m in the material in the first 50 ns of propagation, 1 GHz example ; (right) Peak of the leading transient and the carrier frequency versus propagation length.

where $f(E) = \beta E^3$. This is an approximation to a saturation limited nonlinearity required by our theorem. We implemented the same numerical method outlined above, except that in this case (3.15)-(3.16) contain nonlinear terms. We used a functional iteration in the nonlinear version of (3.15) to obtain e^n , which is then used to update the polarization term p^n . Comparison of the nonlinearly forced model (3.17) with the corresponding linear dynamics is depicted in Figures 4 and 5 for the 10 GHz and 1 THz case, respectively. In these simulations we have a weak nonlinearity with $\beta = -5 \times 10^{-6}$ and the amplitude of the input signal is small, $A = 10$. The linear and nonlinear results do not differ substantially in the 10 GHz case (see Figure 4). In that case if β is positive we observed that a nonlinearly forced polarization dynamics leads to a signal whose main part arrives slightly earlier and is slightly larger than the corresponding portion of the signal in the linear material. More results and comparisons can be found in [7].

In a set of parallel numerical experiments we implemented a nonlinear Debye polarization dynamics given by $\tau \dot{P} + P + sP^3 = \epsilon_0(\epsilon_s - \epsilon_\infty)E$, where s is a small parameter. The cubic nonlinear term is chosen since most biological tissues are not expected to have an axis of symmetry. However, it must be considered as an approximation to a saturation limited nonlinear mechanism that can be anticipated for orientational polarization. Large departures from the linear behavior can be observed even for weak nonlinearities if the amplitude of the input signal is sufficiently large. In our simulations $s = 10^{-3}$ and the amplitude A of the input signal is in the range 10^{10} to 10^{12} . Figures 6 and 7 show the comparison between the nonlinear Debye model and the corresponding linear dynamics in the 10 GHz and 1 THz case, respectively.

In the 10GHz case we find that initially the peak of the transient is attenuated at a faster rate than in the linear case if the amplitude of the input signal is sufficiently large ($\geq 5 \cdot 10^9$). As the propagation continues, the attenuation rate seems to approximate that

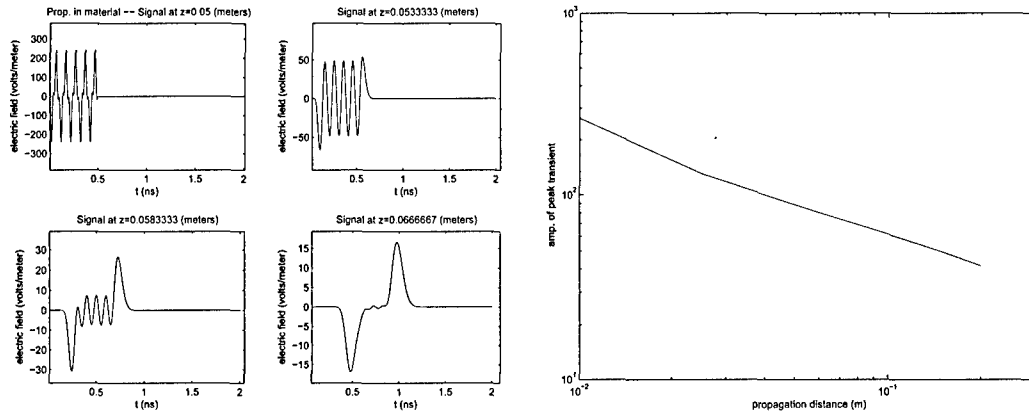


Figure 3: (left) The electric field recorded at the antenna and at 0.0033, 0.00833 and 0.0166 m propagation in the material in the first 2 ns, 10 GHz example ; (right) Peak of the leading transient, loglog plot.

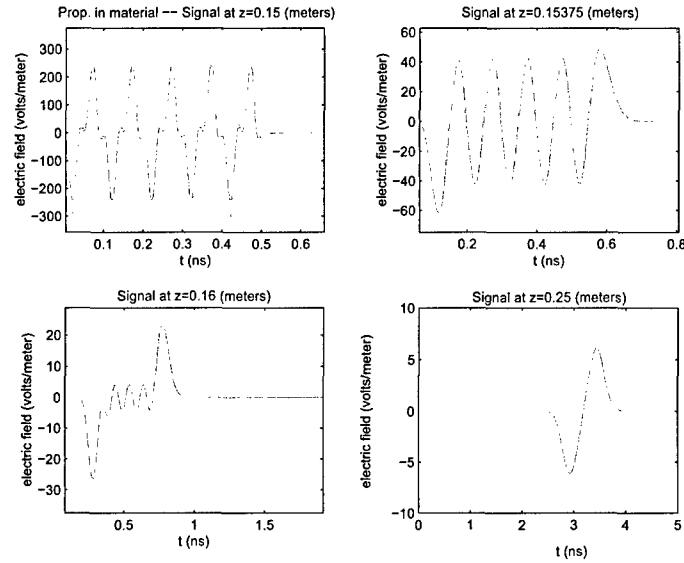


Figure 4: Comparison of the linear (solid line) and nonlinearly forced (dashed line) results, 10 GHz example.

of the linear case. Some of these findings (especially the details of the nonlinear models and corresponding simulations and comparisons with the linear models) are presented in [7].

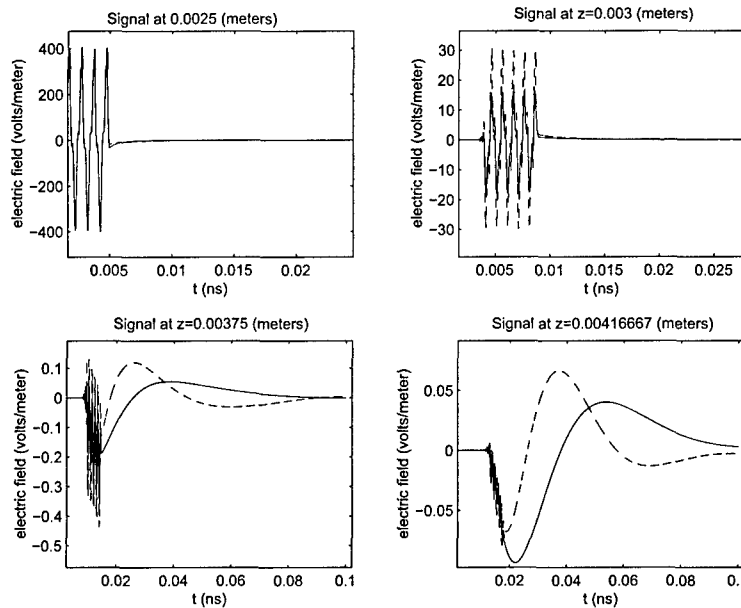


Figure 5: Comparison of the linear (solid line) and nonlinearly forced (dashed line) results, 1 THz example.

4 Models for polymeric materials

As one component in the investigation of the interaction of electromagnetic waves with viscoelastic materials we further developed our models for large dynamic deformations of a polymeric rod. These materials exhibit large hysteresis loops between the stress and strain, which is usually captured by nonlinear constitutive relationships and is thought of as the manifestation of a ‘memory’ in the material. In contrast to our earlier efforts based on a pseudo-phenomenological description of this phenomenon [4, 9] we developed a molecular, i.e., physics based, model that can incorporate the multiscale aspect of the problem. This model is based on a nonlinear extension of the linear reptation models of Doi and Edwards [13] and the work of Johnson and Stacer [14]. We assume that the material consists of physically-constrained and chemically cross-linked molecules whose motion with respect to each other constitutes an ‘internal dynamics’ in the model that contributes to the overall system response. We showed in [5] and [6] that the earlier models of [4, 9] are special cases of this formulation if one considers uniform (or a finite number of) internal dynamics. In the new model we treat a continuum of internal dynamics that are averaged according to a probability distribution. The resulting system is a probability measure dependent partial differential equation for which we established well-posedness in [8]. This approach treats hysteresis as a multiscale phenomenon and is shown to lead to computationally useful approximations [8].

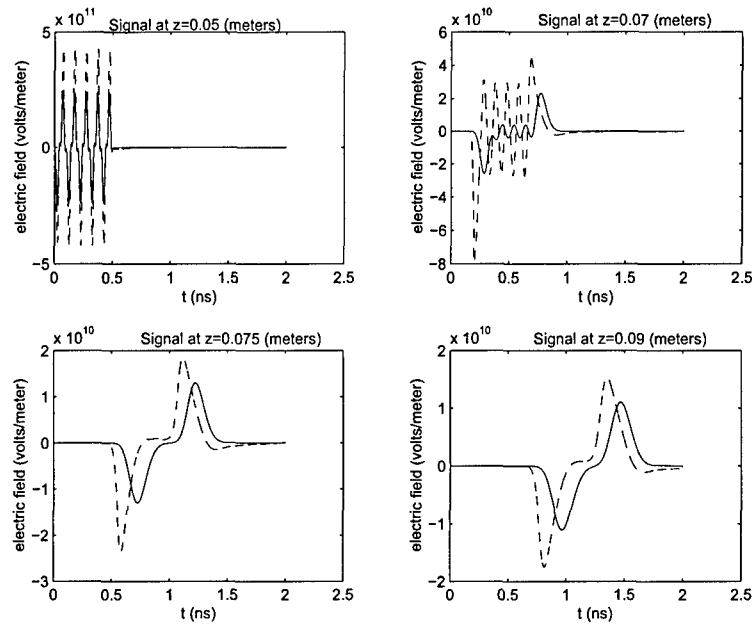


Figure 6: Comparison of the linear (solid line) and nonlinear (dashed line) results, 10 GHz example.

References

- [1] R. Albanese, J. Penn and R. Medina, "Short-rise-time microwave pulse propagation through dispersive biological media", *Journal of the Optical Society of America A*, 9, (1989) p.1441-1446.
- [2] H.T. Banks, M.W. Buksas and T. Lin, *Electromagnetic Material Interrogation Using Conductive Interfaces and Acoustic Wavefronts*, SIAM Frontiers in Applied Mathematics, Philadelphia, 2000.
- [3] H.T. Banks and G.A. Pinter, "Maxwell-systems with nonlinear polarization", *Non-linear Analysis, Real World Applications*, 4, (2003), p.483-501.
- [4] H.T. Banks, M.J. Gaitens, L.K. Potter, G.A. Pinter and L.C. Yanyo, "Modeling of nonlinear hysteresis in elastomers under uniaxial tension," *Journal of Intelligent Material Systems and Structures*, 10, (1999), p.116-134.
- [5] H.T. Banks and G.A. Pinter, A probabilistic multiscale approach to hysteresis in shear wave propagation in biotissue, to appear in *Multiscale Modeling and Simulation* 3 (2005), no. 2, 395-412.

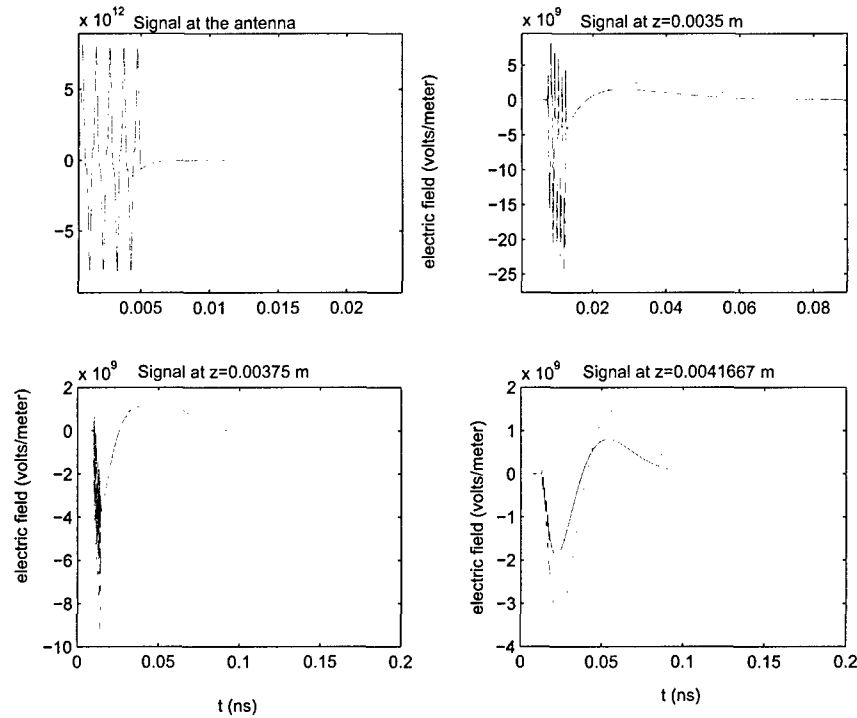


Figure 7: Comparison of the linear (solid line) and nonlinear (dashed line) results, 1 THz example.

- [6] H.T. Banks, N.G. Medhin and G.A. Pinter, 'Nonlinear reptation in molecular based hysteresis models for polymers', *Quarterly of Applied Mathematics*, 62 (2004), no. 4, 767-779.
- [7] H.T. Banks and G.A. Pinter, High frequency pulse propagation in nonlinear dielectric materials, *Nonlinear Analysis: Real World Applications*, 5, (2004) p.597-612.
- [8] H.T. Banks, N.G. Medhin and G.A. Pinter, Multiscale considerations in modeling of nonlinear elastomers, *Journal of Computational Methods in Science and Engineering*, to appear.
- [9] H.T. Banks, L.K. Potter and G.A. Pinter, "Modeling of quasi-static and dynamic load responses of filled viscoelastic materials, in *Modeling: Case Studies from Industry*, E. Cumberbatch and A. Fitt eds., Cambridge University Press, 2001.
- [10] R.W. Boyd, *Nonlinear Optics*, Academic Press, San Diego, 1992.
- [11] P. Günter (ed.), *Nonlinear Optical Effects and Materials*, Springer, Berlin, 2000.
- [12] P. Debye, *Polar molecules*, Chemical Catalog Co., New York, 1929.

- [13] M. Doi and M. Edwards, *The Theory of Polymer Dynamics*, John Wiley & Sons, Inc., New York, 1980.
- [14] A.R. Johnson and R.G. Stacer, "Rubber viscoelasticity using the physically constrained systems' stretches as internal variables," *Rubber Chemistry and Technology*, 66, (1993), p.567-577.
- [15] J.L. Lions, *Optimal Control of Systems Governed by Partial Differential Equations*, Springer-Verlag, New York, 1971.
- [16] A.C. Newell and J.V. Moloney, *Nonlinear Optics*, Addison-Wesley, Redwood City, 1991.
- [17] K.E. Oughstun and G.C. Sherman, "Propagation of electromagnetic pulses in a linear dispersive medium with absorption (the Lorentz medium)," *J. Opt. Soc. Am. B*, 5, (1988), p.817-849.
- [18] Y.R. Shen *Principles of Nonlinear Optics*, Wiley, New York, 1984.
- [19] C. Sulem and P-L. Sulem, *The Nonlinear Schrödinger Equation, Self-Focusing and Wave Collapse*, Springer-Verlag, New York, 1999.
- [20] Wloka, J., *Partial Differential Equations*, Cambridge Univ. Press. 1992.